

An investigation of slow light and time delay-bandwidth in $\text{Pr}^{3+}:\text{Y}_2\text{SiO}_5$
by using the persistent spectral hole burning technique

Master's thesis

By

Nan Lin

Lund Report on Atomic Physics, LRAP-421

Lund, June, 2010

Abstract

This master's thesis evaluates the performance of $\text{Pr}^{3+}:\text{Y}_2\text{SiO}_5$ in slow light by utilizing Persistent Spectral Hole Burning (PSHB), i.e. the extremely slow group velocity as well as the time delay-bandwidth product. A novel method that can be used to measure the high optical depth (αL) value is also tested in $\text{Pr}^{3+}:\text{Y}_2\text{SiO}_5$.

This $\text{Pr}^{3+}:\text{Y}_2\text{SiO}_5$ crystal has many brilliant properties for the slow light aspect, such as its high optical depth and the multipass design, which gives it the potential for obtaining a high time delay-bandwidth. Moreover, the spectral hole is created by spectral hole burning and do not need a strong coupling beam applied simultaneous with the probe beam, which avoids the obstruction to the weak signal.

This thesis gives basic ideas for obtaining a slow group velocity of light and achieving a high time delay-bandwidth by applying PSHB. And the implements in $\text{Pr}^{3+}:\text{Y}_2\text{SiO}_5$ were done in the experiments. Some difficulties and suggestions for solution are discussed. The suggestion of the future work is also given.

Contents

1	Introduction	1
1.1	Outline.	2
2	Slow light	4
2.1	Different definitions for the velocity of light.	4
2.1.1	Phase velocity	4
2.1.2	Group velocity.	5
2.1.3	Energy velocity.	6
2.1.4	Signal velocity.	6
2.2	Different techniques to obtain slow light.	7
2.2.1	Absorption and dispersion.	7
2.2.2	The principle for obtaining slow light.	8
2.2.3	Some methods for slowing the light.	9
2.2.3.1	Electromagnetically induced transparency(EIT).	9
2.2.3.2	Coherent Population Oscillation(CPO).	11
2.2.3.3	Persistent Spectral Hole burning(PSHB).	11
2.2.3.4	Summary.	13
3	Time delay-bandwidth product	15
3.1	Definition of time delay-bandwidth product.	15
3.2	Properties of ideal slow light delay lines.	18
3.3	Properties of EIT/CPO/PSHB slow light delay lines.	19
3.4	High time delay-bandwidth by slow light.	20
4	Rare-Earth-Ion-Doped Crystal	22
4.1	Properties of $\text{Pr}^{3+}:\text{Y}_2\text{SiO}_5$	22
4.2	Spectral hole burning.	24
5	The experimental equipments	25
5.1	The laser system.	25
5.2	Pulse shaping system.	26
5.3	Crystal- $\text{Pr}^{3+}:\text{Y}_2\text{SiO}_5$	27
5.4	Cryostat.	27

6	The experimental methods and setups	29
6.1	High αL measurement.	29
6.1.1	The necessity and the difficulty for knowing high optical depth.	29
6.1.2	A method to measure the αL value of $\text{Pr}^{3+}:\text{Y}_2\text{SiO}_5$	30
6.1.3	The setup of high optical depth measurement	32
6.2	Slow light experiment.	33
6.2.1	To obtain slow light.	33
6.2.2	To obtain high time delay bandwidth product.	33
6.2.3	The setup of slow light.	33
	1) Slow light.	33
	2) High time delay bandwidth product.	34
7	The experimental results and discussions	35
7.1	Test of the method measuring high αL	35
7.1.1	Results.	35
7.1.2	Discussion.	39
7.2	Slow light experiment.	39
7.2.1	Reduce the group velocity of light as much as possible.	39
	1) Result.	39
	2) Discussion.	40
7.2.2	Time delay-bandwidth product experiment.	40
	1) Results.	40
	(a) In the single-pass alignment.	40
	(b) In the multi-pass alignment.	42
	2) Discussion.	42
8	Conclusion and outlook	45
	Acknowledgements	47
	Bibliography	48
	Appendix A The procedure for measuring the αL in $\text{Pr}^{3+}:\text{Y}_2\text{SiO}_5$	50
	Appendix B Adjustment for obtaining multipass in the reflection coated crystal	51

Chapter 1

Introduction

The very good properties of photons make them fabulous carriers of information. Photons have extraordinary rapid speed and they are less susceptible to surrounding interference. Therefore, we can expect photons to be important tools for controlling and transmitting quantum information. Photons can act as the transmission carrier of the wave function between quantum logic gates in quantum computation. Also, they can act as the transmitted or received signal in quantum networks.

When an optical pulse contains a large number of photons, it normally acts as a classical electromagnetic wave. However, light displays a quantum character if the number of photons it contains is less or of the order of a photon. As we know, it is difficult to utilize nonlinear optics to control the information since nonlinear phenomenon only happened at high intensity. The research on slow light effect offers us a method which makes the possibility of nonlinear optics at low intensity. Many applications were aroused by this, for example, multi-wave mixing and all optical switching at weak light intensity. Moreover, the storage of light due to the slow light technology provides a new approach to a quantum memory.^[1] Thus, it is worth to push the research on slow light further. This master's thesis mainly concentrates on the slow light technology.

In people's viewpoint, the speed of light is the fastest in the universe. It seems nothing can succeed the light velocity, not to mention control it. However, this thesis will subvert this kind of

opinion.

Slow light effects were first obtained by the turn of the last century. This area then gained more and more attraction. There are plenty of applications through slow light, for example, optical delay lines and quantum storage.[1] And the record of the slow down factor was rapidly and repeatedly renewed. It is hard to image ultraslow or even frozen light, but people already did that.

Although the group velocity for light pulses could be successfully reduced, the bandwidth of the transparent window was low, and as a result optical buffers based on slow light cannot be used to store much information. The time delay-bandwidth product is a key factor for evaluating the capability of a slow light device. Therefore, a lot of attempts have been done to refresh the time delay-bandwidth product so far. In this thesis, a novel method will be used to obtain a high time delay-bandwidth product using spectral hole burning.

Optical depth or optical thickness (αL) is an important parameter in light-matter interaction. Based on Beer-Lambert Law, $I_{\text{out}} = I_{\text{in}} \cdot e^{-\alpha L}$. Here I_{out} and I_{in} indicate output intensity and input intensity respectively. If αL is large, for example 100, the output intensity is decreased by factor 3.7×10^{-44} . That means that we cannot directly measure the value of αL by measuring the transmitted intensity. In this thesis a method which is suitable for measuring high values of αL will be presented.

1.1 Outline

This thesis is structured as follows.

Chapter 2 and 3 give the background knowledge of my work. In Chapter 2 the theory for slow light is developed, leading to expressions for the different definitions of light velocities, some methods for obtaining slow light as well as their records. Chapter 3 highlights the time delay-bandwidth product. The definition and the properties are introduced.

Chapter 4, 5 and 6 are devoted to describe the materials, equipments and techniques that are using in the experiment. In Chapter 4, the properties related to the experiments are introduced.

The explanations of the experimental equipments are given in Chapter 5. The experimental methods and setups are provided in Chapter 6.

Chapter 7 presents the results and discussions.

Finally, the conclusions of the experiments are come out in Chapter 8 as well as the outlook for the future.

Chapter 2

Slow Light

In this chapter, some basic concepts will be explained. First, I will describe several different ways to define the velocity of light. Then methods used to reduce the group velocity and experimental results from each method will be presented.

2.1 Different definitions for the velocity of light

As discussed in special relativity, the speed of light is limited by the value of c . However, there are several experiments obtained the velocities of light which are large than c . Was Einstein wrong? Therefore, it is worth to understand the different definitions of velocities before we make the conclusion.

2.1.1. Phase Velocity[2]

For a monochromatic plane wave φ in a lossless, homogeneous and isotropic medium, assuming that the wave propagates along the x axis, the wave can be described as

$$\varphi = Ae^{i(kx-\omega t)} \quad (2.1)$$

Where A is amplitude, k is wave number, ω is angular frequency and t is time. For the point that is moving at a velocity such the phase is fixed, $kx - \omega t = \text{constant}$. Thus,

$$V_p = \frac{dx}{dt} = \frac{\omega}{k} \quad (2.2)$$

Where v_p is the speed at which the phase of the wave travels in space, called phase velocity.

2.1.2. Group Velocity^[2]

Phase velocity of a monochromatic wave is constant in a non-dispersive medium. In a dispersive medium, however, the phase velocity depends on the frequency. Because different frequency components of the wave move at different velocities, that induces a 'diffusion' of the wave. Assuming this wave is comprised by harmonic waves, which have a tiny frequency difference between each other, will propagate as an entirety in a certain speed. The special group of waves named wave packet, and speed of that is group velocity. See the [figure 2.1](#).

The group velocity is defined as

$$v_g = \frac{d\omega}{dk} \quad (2.3)$$

Consider two interfering waves with slightly different frequencies and wavelengths

$$A(x, t) = \cos[(k - \Delta k)x - (\omega - \Delta\omega)t] + \cos[(k + \Delta k)x - (\omega + \Delta\omega)t] \quad (2.4)$$

Which can be rewritten as

$$A(x, t) = 2 \cos(kx - \omega t) \cos(\Delta kx - \Delta\omega t) \quad (2.5)$$

As a result, the two waves can be expressed as one amplitude modulated wave. [Figure 2.1](#) is an example of such a resulting amplitude modulation. The speed of the envelope is the group velocity.

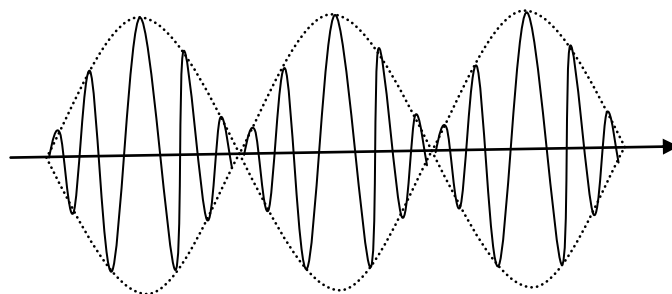


Figure 2.1 Envelop of different frequency components.

2.1.3. Energy Velocity^{[3][4]}

Each wave carries energy. During the transmission of an electromagnetic wave, the energy is also flowing in the space followed by the wave. The speed of this energy flow called energy velocity.

2.1.4. Signal Velocity

In Einstein's special relativity, there is no signal can travel faster than the speed of light. However, the group velocity of light pulses that faster than c was obtained in experiment. To understand this, we need to know what Einstein really means by 'signal'.

In Ref. [3], a definition for signal velocity was given, which is consistent with Einstein's requirement. The signal was mentioned there is a signal with a sharp switch-on or cut-off. That means that it is not continuous all along the optical pulse, which has a discontinuity as the figure 2.2 shown.

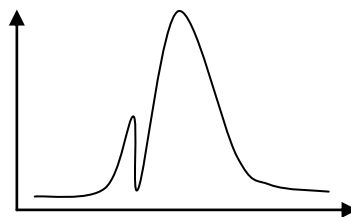


Figure 2.2 Gaussian pulse with a discontinuity

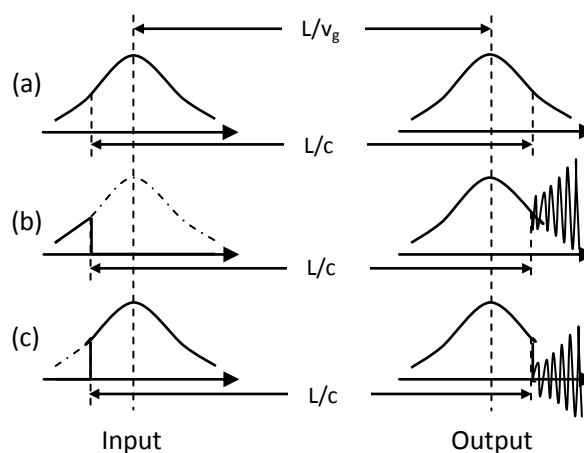


Figure 2.3 The incident signals and the transmitted signals passed a medium of L meters. ($v_g > c$)

(a) shows a normal Gaussian shape pulse. (b) indicates a cut off in the early stage of the Gaussian pulse. (c) expresses a contrary way to cut off compare to (b)^[5]

The explanation on the impossibility that the speed of this discontinuity cannot exceed the speed of light was done in Ref. [5]. The gaussian pulses travel at a group velocity which is larger than c can be presented as figure 2.3(a). If there is a cut-off at an early stage of the pulse, see figure 2.3(b), the transmitted pulse remains the shape until t_0+L/c , where the oscillation starts. If we cut off the pulse in another way but still in the same time as before in figure 2.3(c), the oscillation will start at t_0+L/c too. (According to Eq.(11) in Ref. [5]) That means that the discontinuity of the pulse cannot exceed c , although the group velocity is larger than c .

In the slow light technique which will be mentioned later, the materials will always have normal dispersion. ($\frac{dn}{d\omega} > 0$) In this case, the group, signal, energy velocities coincide and the value of that is smaller than the phase velocity.

2.2 Different techniques to obtain slow light

The description will be focused on the different techniques which have been used in slow light demonstration so far. Before that the basic principle on Kramers-Kronig Relations and the idea about how to obtain slow light will be explained. The different methods then will follow. In the end, a comparison of different ways is made in a summary part.

2.2.1 Absorption and Dispersion

The complex susceptibility has real and imaginary parts, which can be described as

$$\chi = \chi'(v) + j\chi''(v) \quad (2.6)$$

The relation between absorption and dispersion is intertwined, which can be expressed through the relation between real and imaginary parts of the susceptibility. The famous relation between $\chi'(v)$ and $\chi''(v)$ called Kramers-Kronig Relations[6]:

$$\chi'(v) = \frac{2}{\pi} \int_0^{\infty} \frac{s\chi''(s)}{s^2-v^2} ds \quad (2.7)$$

$$\chi''(v) = \frac{2}{\pi} \int_0^{\infty} \frac{v\chi'(s)}{v^2-s^2} ds \quad (2.8)$$

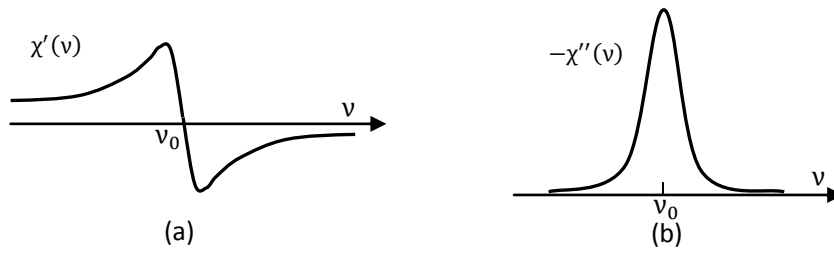


Figure 2.4 The real and imaginary parts of the susceptibility of a resonant dielectric medium.[2]

If a medium with refractive index n_0 is a host to impurities, and if there are resonant impurity atoms that are sufficiently dilute ($\chi'(\nu) \ll 1, \chi''(\nu) \ll 1$), the refractive index and absorption coefficient are given by[2]

$$n(\nu) \approx n_0 + \frac{\chi'(\nu)}{2n_0} \quad (2.9)$$

$$\alpha(\nu) \approx -\left(\frac{2\pi\nu}{n_0 c_0}\right) \chi''(\nu) \quad (2.10)$$

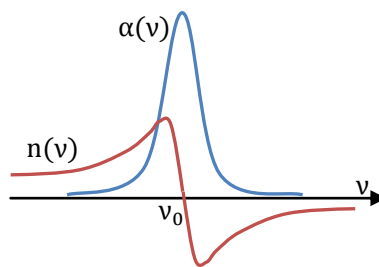


Figure 2.5 The absorption coefficient and refractive index as a function of frequency

2.2.2 The principle for obtaining slow light[2]

Monochromatic light travels at the phase velocity, which depends on the refractive index in the medium.

$$v_p = \frac{\omega}{k} = \frac{c}{n} \quad (2.11)$$

The refractive index depends on the angular frequency, $n = n(\omega)$. A realistic wave is a wavepacket which consists of many frequency components. That means that when the

wavepacket goes through a dispersive medium, there are various velocities for different frequencies since these have different refractive indexes. Therefore, we cannot use the phase velocity to analyze the movement of the wavepacket. We need to define another velocity for that, which is group velocity.

From the definition of group velocity:

$$v_g = \frac{d\omega}{dk} = \frac{c}{n_g} \quad (2.12)$$

And

$$n_g = n(\omega) + \omega \frac{dn(\omega)}{d\omega} \quad (2.13)$$

Then we can have the relationship between group velocity and refractive index.

$$v_g = \frac{c}{n(\omega) + \omega \frac{dn(\omega)}{d\omega}} \quad (2.14)$$

Where c is the speed of light in vacuum, $\omega = 2\pi\nu$ is the angular frequency, $n(\omega)$ is refractive index of that frequency component in the medium.

It is not hard to see that the group velocity can be decreased by increasing the denominator. The frequency dependent of the refractive index ($n(\omega)$) is small. However, the second part of the denominator ($\omega dn/d\omega$) can be significant. Therefore, if we can get a great positive derivative ($dn/d\omega$), then the group velocity will be reduced.

2.2.3 Some methods for slowing the light

2.2.3.1 Electromagnetically induced transparency

Electromagnetically induced transparency (EIT) is one of the frequently used methods for producing slow light. From the Kramers-Kronig relations, we can find that a change in absorption coefficient induces a change in refractive index. Therefore, if there is a narrow absorption hole made by EIT, there must be a sharp change on the refractive index. This rapid change produces a great and positive derivative, then slow light achieved.

The probe light is what we want to measure, and ν_p is the frequency of that. When the probe

light goes through the medium, it will be absorbed so that the atoms transit from $|1\rangle$ to $|3\rangle$, see [figure 2.6](#). Due to the fact that the probe light is absorbed by atoms, the signal intensity after propagates through the medium will be weakened. However, we are usually interested in the resonance frequency region which has huge absorption since the potential for making extremely slow light. Therefore, we need a method to transmit the pulse although the absorption is very high. In 1990, Harris formally launched the definition of EIT[\[7\]](#). A strong coupling light whose frequency is tuned as that between $|2\rangle$ and $|3\rangle$ is used for this purpose. As a result, $|1\rangle$ and $|2\rangle$ become superposed coherent states: $|1\rangle - \Omega_p/\Omega_c|2\rangle$, where Ω_p and Ω_c express the rabi frequencies of probe light and coupling light respectively, and they have certain phase difference between each other. This superposed state is called 'dark state'.[\[8\]](#) Because in such a state the two transitions at which light can be absorbed have destructive interference so that neither probe light nor coupling can be absorbed. The destructive quantum interference ensures that no atoms can be excited to the excited state, so the absorption coefficient is reduced to zero.

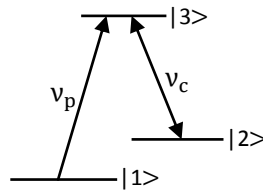


Figure 2.6 Three levels in Λ system

Electromagnetic induced transparency has been the technique mainly used for slow light. Based on this, some groups got very exciting results. In 1999, Lene Vestergaard Hau's group reduced the group velocity to 17m/s[\[9\]](#), which around 60km/h. This is also the average speed in the Tour de France. The medium they used is a gas of sodium atoms cooled to nanokelvin temperatures. In this extremely low temperature, almost every atom is located in the ground state $|1\rangle$ so that there were no atoms in other states ($|2\rangle$ and $|3\rangle$). By applying the EIT technique, normal dispersion with great derivative occurred at the region near the resonance. Therefore, slow group velocity was achieved, see Eq. (2.14).

Subsequently, Michael M.Kash et al. obtained the group velocity in a gas of rubidium atoms.[\[10\]](#) The work was done in a hot atomic gas and the coupling light parallelly propagated as the probe light this time instead of orthogonal propagation in L.V.Hau's experiment. Next, Budker D. et al.

obtained 8m/s by using the same method.[11] Then, Turukhin A. V. et al. observed a speed of 45m/s in solid medium at 5K.[12]

Although EIT achieved remarkable records on slow light, there are some limitations. EIT needs very accurate quantum interference between two amplitudes, even small collisions can destroy the interference. That is why EIT requires the medium be a gas with low atomic density or solid cooled at an extremely low temperature. Thus we cannot use solid materials as the medium to observe slow light by using EIT at room temperature.

2.2.3.2 Coherent Population Oscillation

S. E. Schwartz and T. Y. Tan predicted the existence of a transmission hole because of coherent population oscillations (CPO).[13] Subsequently, it was widely discussed and used for slowing the light.[14][15]

The principle of coherent population oscillations is that when strong coupling light and weak probe light which have different frequencies interact in a saturable absorber, the population of ground state will oscillate in time with the beating frequency of the two input beams. If the angular frequency of the strong coupling light is ω_c and that of the weak probe light is ω_p . The beat frequency of the two waves is $\delta = (\omega_p - \omega_c)/2\pi$. T_1 indicates the life time of excited state. If δ is smaller than $1/T_1$, the oscillation becomes significant. When $\omega_c \rightarrow \omega_p$ or $\delta \rightarrow 0$, a narrow hole will appear in the absorption of the probe. And the width of that is inverse proportional to T_1 . [13]

In 2003, Matthew S. Bigelow et al. obtained group velocity as low as 57.5 ± 0.5 m/s in Ruby crystal at room temperature. That is the first time that slow light was successfully achieved in solid at room temperature.[14] E. Baldit et al. got a velocity of 2.7m/s in $\text{Er}^{3+}:\text{Y}_2\text{SiO}_5$ at 1.5K by using CPO soon after.[15]

The main advantage for CPO is that can be used in solid at room temperature, which makes it more realistic to be applied in practical.

2.2.3.3 Persistent Spectral Hole Burning

From the description of EIT and CPO, it is easily found that a strong pump light needs to be sent

synchronously with the signal light. Sometimes, the strong beam may obstruct the detection of the weak signal. In the Persistent Spectral Hole Burning (PSHB) scheme, the steep derivative in the refractive index profile is created by a beam which is not simultaneous with the probe beam.

The inhomogeneous absorption linewidth is much wider than the homogeneous linewidth in rare-earth-ion-doped crystals. Here, the homogeneous linewidth is the resonance linewidth of individual ions and the inhomogeneous linewidth is the total linewidth over all of the ions and their frequency distribution. By using a narrow linewidth laser, it is possible to selectively excite ions absorbing at a particular frequency. This kind of selective excitation can make an 'empty pit' in the inhomogeneous broadening profile, due to the decrease of absorption at that frequency.

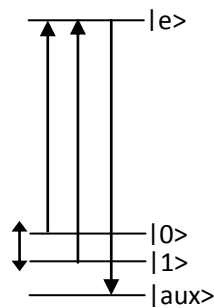


Figure 2.7 The inhomogeneous $^1D_2-^3H_4$ absorption line in $Pr^{3+}:Y_2SiO_5$.

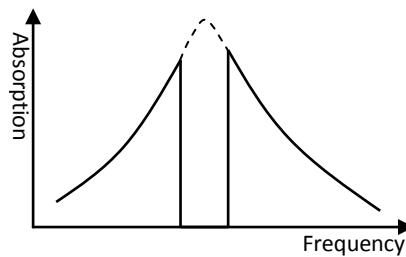


Figure 2.8 Spectral hole appears in absorption profile after laser burning.

The principle of optical pumping can be understood like this. If the laser is scanned over ground states $|0\rangle$ and $|1\rangle$, the ions will be excited to the excited state. After the lifetime T_1 , atoms will decay back to the ground states. However, if the laser remains tuned to this frequency, the atoms will be re-excited if they fall. Thus, they will eventually be removed to another ground state. Therefore, a non absorption hole will be made. The velocity after slowed down is basically described by

$$v_g = 2\pi\Gamma/\alpha \quad (2.15)$$

Where Γ is the width of the hole and α is the absorption coefficient out of the hole. By using this equation, the result of the experiment can be evaluated. More information can be found in Refs. [16][17][18]. By utilizing this method, R. Lauro et al. had a speed 2500m/s. [19]

The inhomogeneous broadening is 5GHz and the homogenous linewidth is only 1kHz in the experimental crystal as will be presented later. This makes it possible to make several holes in the inhomogeneous absorption profile, which gives the potential to implement multi-channel optical storage.

2.2.3.4 Summary

Slow light can be obtained when the derivative $dn/d\omega$ is large. From the Kramers-kronig relations, the derivative will be positive, when there is a 'hole' in the absorption profile. The value of the derivative is inversely proportional to the width of the hole, meanwhile it is proportional to the depth of the hole. That means that extremely slow velocity can be achieved if we can make such a hole in the absorption profile. The relation between the absorption and the refractive index is shown in Figure 2.9. The hard solid lines in the figure represent the situation without any hole-made mechanism, while the dotted lines indicate that after the hole appeared. It is not hard to find that there is a precipitous and positive derivative at the region near the resonance frequency. Therefore, slow light will be produced.

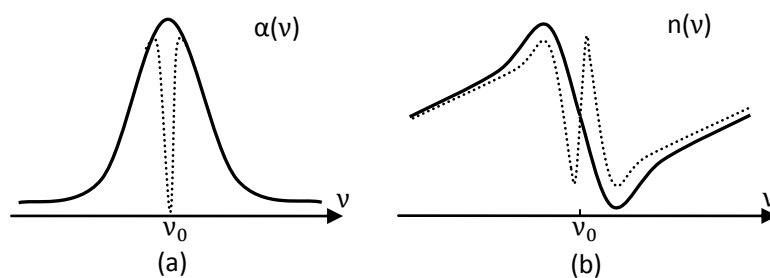


Figure 2.9 The relation between absorption and refractive index from Kramers-Kronig Relations

A comparison is made among the three ways to produce slow light described above, which can be seen in table 2.1. In the experiment I will present later, the method which will be used is Persistent Spectral Hole Burning.

Table 2.1 Comparison of three schemes in slow light

Method	Advantage	Disadvantage	Some Records
EIT	The width of the EIT hole can be made very narrow, of the order of 10kHz. Thus, it is suitable for high resolution spectroscopy.	Cannot be implemented in solid at room temperature, because quantum interference is easily influenced by collisions.	In gas: 17m/s(nK) 8m/s(warm) In solid: 45m/s(5K)
CPO	Can be used in solid at room temperature, which gives it a potential in telecommunication network.	Still needs to shine pump light and probe light at the same time.	In solid: 57 ± 0.5 m/s(room temperature) 2.7m/s(1.5K)
PSHB	Only one beam is sent to the medium at one time, which makes it simple to implement in the experiment.	Also need the cryogenic temperature to implement.	In solid: 2500m/s(1.8K)

Chapter 3

Time delay-bandwidth Product

Slow light can be used in slow light delay lines or buffers, which are crucial components for future all-optical network. Time delay-bandwidth product is an important index to evaluate the capacity of optical delay lines. It is shown that slow light delay lines have limited capacity and time-delay bandwidth. In theory and experiment, group velocity can be reduced to approach zero. From equation (2.15), extremely slow light usually accompanies a very narrow bandwidth Γ , which means the inverse fourier transform cannot be narrow. In telecommunication, however, short duration pulses are usually needed. Thus, one focus of current research is to increase the bandwidth. There is a tradeoff between time delay and bandwidth, which is needed to be optimized. In this chapter, the importance of time delay-bandwidth will be highlighted.

3.1 Definition of time delay-bandwidth product

Time delay-bandwidth is expressed as end-to-end time delay (in seconds) multiplied by the bandwidth (bits/s), which indicates the number of bits the transmitter must send before the first bit arrives at the detector. Moreover, the unit of the result of the product is in bits.[20] The product represents the maximum data can be hold in the device at a certain time.

$$\text{DBP} = \text{Time delay} \times \text{Bandwidth}$$

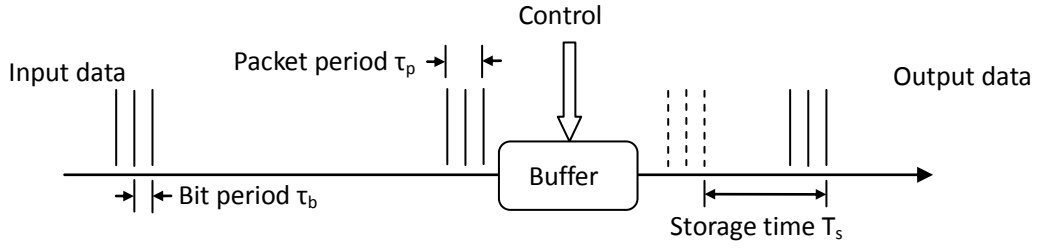


Figure 3.1 Optical buffer[20]

Here, we analyze an optical buffer with length L . The input data has many packets with frequency centered at ω_0 . The length of each bit is τ_b , and that of each packet is τ_p . The baseband bandwidth of each packet is

$$B_{\text{packet}} \cong \frac{1}{\tau_b} \quad (2.16)$$

And the width of the packet is

$$\Delta\nu = \frac{\Delta\omega}{2\pi} \approx 2B_{\text{packet}} \quad (2.17)$$

As Figure 3.1 shown, the time distance between control added and no control added is the storage time of the buffer. The solid lines represent the situation without control, and the dashed lines indicate that a control pulse is applied. Then the time delay-bandwidth product can be described as

$$\text{DBP} = T_s \cdot B_{\text{packet}} = \frac{T_s}{\tau_b} = C \quad (2.18)$$

Note that the time delay-bandwidth is equivalent to the number of bits can be stored in the buffer, which represents the capacity.

An optical buffer is supposed to merely slow down light when the control signal is added. If there is no control signal, it does nothing except let light go through as indicated in Figure 3.1. This effect of the buffer is expressed as Figure 3.2 below. V_{g1} and V_{g2} separately denote the speed with or without control signal.

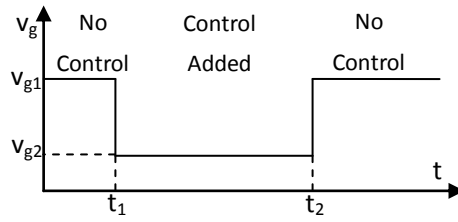


Figure 3.2 The diversification of group velocity in a buffer

The group velocity is described as equation (2.14). Thus, the deceleration factor can be gained by

$$D(\omega) = \frac{v_{g1}}{v_{g2}} = \frac{\frac{c}{n_1(\omega) + \omega \frac{dn_1(\omega)}{d\omega}}}{\frac{c}{n_2(\omega) + \omega \frac{dn_2(\omega)}{d\omega}}} = \frac{n_2(\omega) + \omega \frac{dn_2(\omega)}{d\omega}}{n_1(\omega) + \omega \frac{dn_1(\omega)}{d\omega}} = \frac{n_{g2}}{n_{g1}} \quad (2.19)$$

In most cases, $\omega(dn_1/d\omega) \approx 0$. Therefore, the slow-down factor is dominating determined by $\omega(dn_2/d\omega)$. The $\omega(dn_2/d\omega)$ should not only have a sharp slope, but also be independent of frequency across the passband bandwidth. That is because we consider low distortion propagation as well as the slow-down factor. As a result, that requires a straight line with large slope as in [Figure 3.3](#).

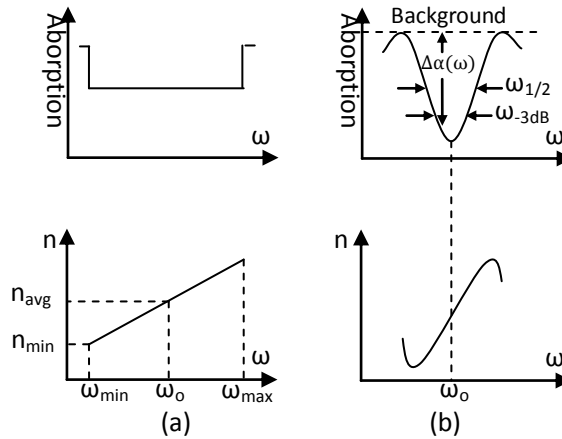


Figure 3.3 Characteristics of slow light delay lines[21]

We expect the derivative $(dn/d\omega)$ as large as possible. Moreover, the linear region in the frequency domain is needed to be maximized due to the requirement for minimizing the distortion. [Figure 3.3\(a\)](#) shows the characteristics of ideal delay line. It has constant absorption that independent of frequency, which means different frequency components of a light wave will be absorbed equally. In addition, the refractive index remains linear over the full signal passband,

which avoids the distortion because of different group velocities of different frequencies. The purpose of illustrating the ideal case is to provide an understanding of the best situation possible and the ideal delay line can supply us with a reference for evaluating the performance of practical delay lines.

Figure 3.3(b) shows the characteristic by using EIT/PO/SHB. There is a spectral hole in the center of the absorption profile, which is not flat all the time as that in Figure 3.3(a). And the linear region in the figure that shows the refractive index as a function of frequency is not as wide as that in Figure 3.3(a). The limitation for this is from the Kramers-Kronig Relations. The linear region only aroused at the frequencies where the hole was made. Thus, the conclusion is that the non-constant absorption limits the bandwidth.

Next, the characteristics of each ideal delay line or practical one will be explained and calculated respectively. In contrast, we can recognize the limitation.

3.2 Properties of ideal slow light delay lines

The derivative which significantly influences the group velocity in this case is

$$\frac{dn}{d\omega} = \frac{n_{\max} - n_{\min}}{\omega_{\max} - \omega_{\min}} = \frac{2(n_{\text{avg}} - n_{\min})}{\omega_{\max} - \omega_{\min}} \quad (2.20)$$

The deceleration factor can be calculated through (2.19). In most cases, $dn_1/d\omega=0$. $\omega \approx \omega_0$, $n_2(\omega) \ll 2\omega(n_{\text{avg}} - n_{\min})/\Delta\omega$ and $k=2\pi/\lambda=\omega/c$. Then (2.19) can be simplified like below

$$D_{\text{ideal}}(\omega) = \frac{n_2(\omega) + \omega \frac{dn_2(\omega)}{d\omega}}{n_1(\omega) + \omega \frac{dn_1(\omega)}{d\omega}} = \frac{\omega \frac{2(n_{\text{avg}} - n_{\min})}{\Delta\omega}}{n_1} = \frac{2c(n_{\text{avg}} - n_{\min})}{n_1 \lambda_0 \Delta\nu} \quad (2.21)$$

Where λ_0 is the wavelength of at the center of the bandwidth. The group velocity is

$$V_{g2} = \frac{v_{g1}}{D(\omega)} = \frac{\lambda_0 \Delta\nu}{2(n_{\text{avg}} - n_{\min})} = \frac{\lambda_0 B_{\text{packet}}}{(n_{\text{avg}} - n_{\min})} \quad (2.22)$$

From this formula, the trade off relation between the deceleration factor and the bandwidth comes out. B_{packet} which reveals the bandwidth is inverse proportional to the deceleration factor $D(\omega)$.

The delay time is the parameter considered next.

$$T_{\text{ideal}} = \frac{L}{v_{g2}} - \frac{L}{c} \quad (2.23)$$

If $V_{g2} \ll c$, then

$$T_{\text{ideal}} = \frac{L}{v_{g2}} = \frac{2L(n_{\text{avg}} - n_{\text{min}})}{\lambda_0 \Delta v} \quad (2.24)$$

The time delay-bandwidth which also implies the capacity of the delay line is

$$\text{DBP} = C_{\text{ideal}} = T_{\text{ideal}} \cdot B_{\text{packet}} = \frac{L(n_{\text{avg}} - n_{\text{min}})}{\lambda_0} \quad (2.25)$$

3.3 Properties of EIT/PO/SHB slow light delay lines

The deceleration factor is firstly considered here.

The absorption coefficient and refractive index have a relation [1] as

$$n - \frac{\alpha}{2k_0} j = \sqrt{\frac{\epsilon}{\epsilon_0}} = \sqrt{1 + \chi' + j\chi''} \quad (2.26)$$

Where n demonstrates the refractive index, and $\epsilon = \epsilon/\epsilon_0$ represents the dielectric constant.

Thus, the real part of $\sqrt{\epsilon}$ corresponds to the refractive index. From (2.19), the deceleration factor is

$$D(\omega) = \frac{n_2 + \omega \frac{dn_2(\omega)}{d\omega}}{n_1} = \frac{n_2}{n_1} + \frac{\omega d\text{Re}\epsilon(\omega)}{2n_1 n_2 d\omega} \quad (2.27)$$

Via Kramers-Kronig Relations the real part of ϵ can be denoted

$$\text{Re}\epsilon(\omega) = 1 + \frac{1}{\pi} P \int_{-\infty}^{+\infty} \frac{\text{Im}\epsilon(\omega')}{\omega' - \omega} d\omega' \quad (2.28)$$

Where the P in front of the integral is to remove the singularity and is defined as

$$P \int_{-\infty}^{+\infty} \frac{1}{\omega' - \omega} d\omega' = \lim_{\epsilon \rightarrow 0^+} \left(\int_{-\infty}^{a-\epsilon} \frac{1}{\omega' - \omega} d\omega' + \int_{a+\epsilon}^{+\infty} \frac{1}{\omega' - \omega} d\omega' \right) \quad (2.29)$$

Then the deceleration factor can be expressed by combining both (2.27) and (2.28).

$$D(\omega) = \frac{n_2}{n_1} + \frac{\omega}{2\pi n_1 n_2} P \int_{-\infty}^{+\infty} \frac{\text{Im}\varepsilon(\omega')}{(\omega' - \omega)^2} d\omega' \quad (2.30)$$

$\Delta\alpha(\omega)$ is defined as the absorption attenuation compare to the maximum absorption. And the hole shape is a Lorentzian. Therefore, $\Delta\alpha(\omega)$ can be denoted as

$$\Delta\alpha(\omega) \approx \frac{\Delta\alpha_0(\omega)}{1 + \left(\frac{2\delta}{\omega_{1/2}}\right)^2} \quad (2.31)$$

Where $\delta = (\omega - \omega_0)$ is the detuning and $\omega_{1/2}$ is the full width half maximum of the hole bandwidth. Moreover, $\Delta\alpha(\omega)$ can be known also from Kramers-Kronig Relations[1].

$$\Delta\alpha(\omega) = \frac{-\omega \text{Im}\varepsilon(\omega)}{n \cdot c} \quad (2.32)$$

Substituting (2.31) and (2.32) into (2.30)

$$D(\omega_0) = \frac{n_2}{n_1} + \frac{c\Delta\alpha(\omega_0)}{n_1 \omega_{1/2}} \quad (2.33)$$

Thus, the deceleration factor is obtained.

The delay time which is indicated by (2.24) when $v_{g2} \ll v_{g1}$.

$$T = \frac{L}{v_{g2}} = L \left(\frac{n_2}{c} + \frac{\Delta\alpha(\omega_0)}{\omega_{1/2}} \right) \quad (2.34)$$

Because the slow down factor is usually large, the second term has the larger impact on the delay time. That means that the first term in (2.34) can be ignored.

The time delay- bandwidth product is

$$\text{DBP} = T \cdot B_{\text{packet}} = T \cdot \frac{\Delta\nu}{2} = T \cdot \frac{\omega_{1/2}}{4\pi} = \frac{\Delta\alpha(\omega_0) \cdot L}{4\pi} \quad (2.35)$$

3.4 High time delay bandwidth by slow light

High time delay bandwidth indicates a better capability to keep information, which is the core of research on slow light recently. From the experiments by using Electromagnetically Induced Transparency or Coherent Population Oscillation, the time delay-bandwidth product was not desirable. For example, the time delay bandwidth products are 2 from Ref[22] and 1 from Ref[23]

respectively. That means that the devices used for delaying light only have 1 or 2 bits' memory. However, the electronic routers have the capacity of around 10Gb. In order to replace those by optical ones, there is long way to go.

In contrast, Spectral Hole Burning usually has a larger $\Delta\alpha(\omega_0) \cdot L$ in (2.35), which gives it a potential to obtain a higher time delay-bandwidth product. The experimental part in this thesis is an attempt to demonstrate this.

Chapter 4

Rare-Earth-Ion-Doped Crystal

This chapter is dedicated to elucidate the properties of the hardware for quantum memory which is related to the experiments. The crystal that has been used is a kind of rare-earth-ion-doped crystal, i.e. $\text{Pr}^{3+}:\text{Y}_2\text{SiO}_5$. A full description of the properties of this material will be restricted to those important for the next chapters.

4.1 Properties of $\text{Pr}^{3+}:\text{Y}_2\text{SiO}_5$

Praseodymium belongs to the Lanthanides which, e.g., can be doped into $\text{Y}_3\text{Al}_5\text{O}_{12}$ (YAG) or Y_2SiO_5 (YSO). Pr ions will replace the host ions in the crystal lattice randomly. The local electric field of the ions depends on their neighboring ones. The homogenous linewidth of Pr is narrow, just a few kilo hertz. However, due to the random surrounding which induces slightly different energy levels shift, there is an inhomogenous broadening. As a result, a linewidth with a magnitude of several giga hertz appears. By accurately controlling the linewidth of the laser, ions with a selected specific frequency can be selected. Moreover, the large number of ions at any given frequency gives the probability for achieving multi-mode memory. [28]

The surrounding of Pr ions is slightly different as indicated in [figure 4.1](#). And the absorption frequency of a Pr ion when embedded in the crystal is determined by the local electric and magnetic fields. Different ions will absorb different frequencies, as the [figure 4.2](#) shown.

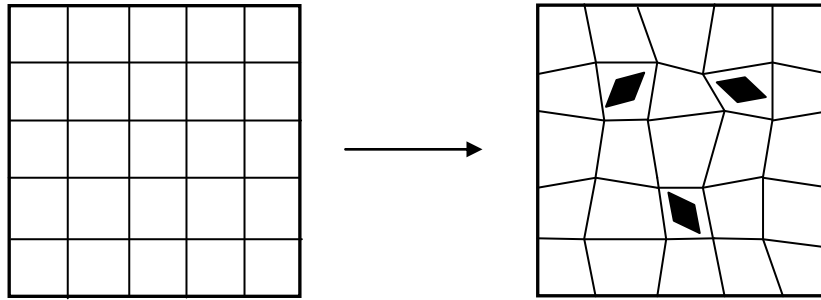


Figure 4.1 The surrounding of each Pr ions is slightly different after doping

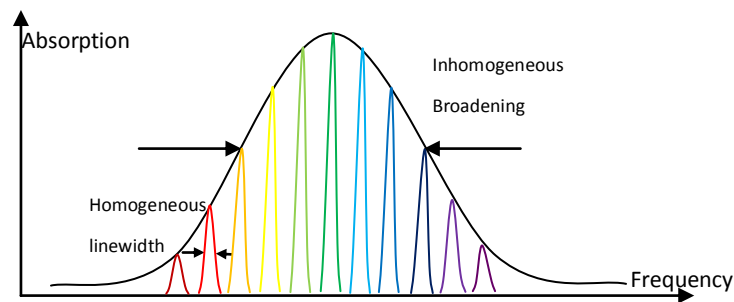


Figure 4.2 The homogeneous linewidth and the inhomogeneous broadening

The transition wavelength between the 3H_4 and 1D_2 states is 605.82nm in $Pr^{3+}:Y_2SiO_5$. And each energy level is split into three hyperfine levels. The hyperfine levels can be represented like figure 4.3. The lifetime of the hyperfine levels can be large, around 100s. Moreover, the coherence property of the crystal is good at cryogenic temperature, it is 500 μ s at zero magnetic field.[24][25]

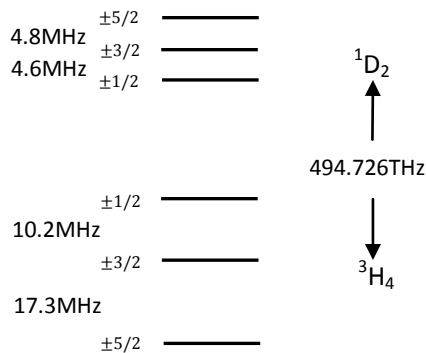


Figure 4.3 The relevant hyperfine levels of Pr^{3+}

4.2 Spectral hole burning

In this project, slow light is obtained by using spectral hole burning. To be able to achieve this, a laser with narrow linewidth is first scanning back and forth in a defined frequency region. The ions in this frequency interval are removed to other states. After tailoring a narrow spectral hole in the absorption profile, the slow light will be gained based on Kramers-kronig relations.

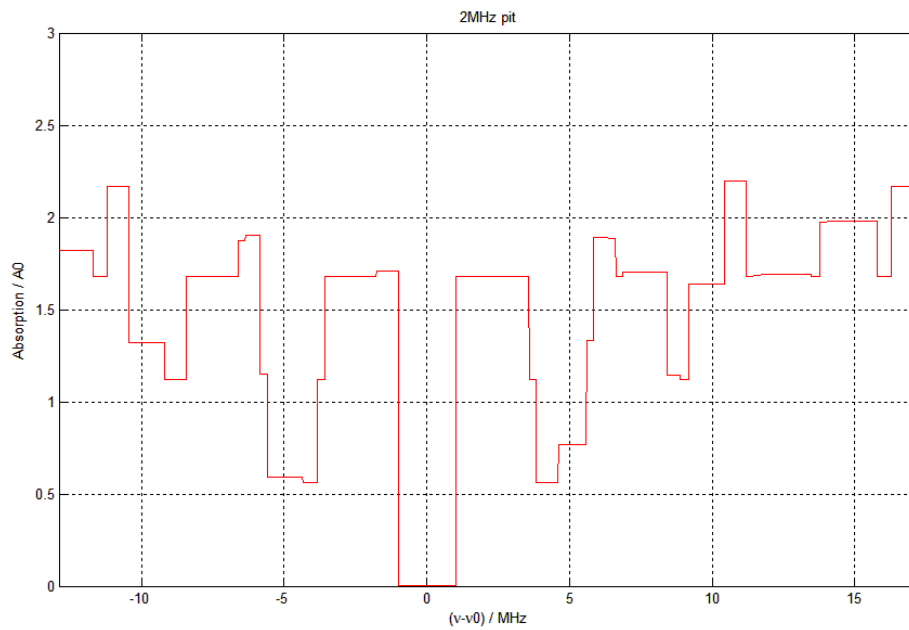


Figure 4.4 A 2MHz pit which will be used in the experiment

Chapter 5

The experimental equipments

The instruments which have been used in the experiments will be presented, such as the laser source with a stabilization system, the pulse shaping system and the cryostat. In addition, the setups that implement the experiments will be developed and described.

5.1 The laser system

A continuous wave ring cavity dye laser (Coherent 699-21) is used in this project. This is pumped by a Nd:YVO₄ solid state laser (Coherent Verdi V6) at 532nm with pump power 6W. The active medium is Rhodamine 6G, which can be tuned to 606nm. The dye is cooled to 8°C and its pressure when entering the dye nozzle is 4.2bar. The output intensity of this laser system can in the present experiments typically is 400-600mW.

Due to the demand for fine controlling the ions in a particularly narrow frequency interval, a laser stabilization system was constructed.[\[26\]](#)[\[27\]](#) This unique stabilization system is different from normal cavity locking, instead it is using a spectral hole burning technique.[\[27\]](#) Without this external locking, the linewidth can be kept about 1MHz by the internal locking from the original dye laser stabilization system. After applying the external stabilization feedback, the linewidth is narrowed to 1kHz. The schematic view of the laser stabilization system is shown in [figure 5.1](#).

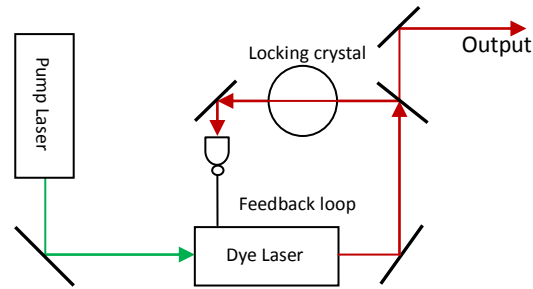


Figure 5.1 Laser frequency stabilization system

5.2 Pulse shaping system

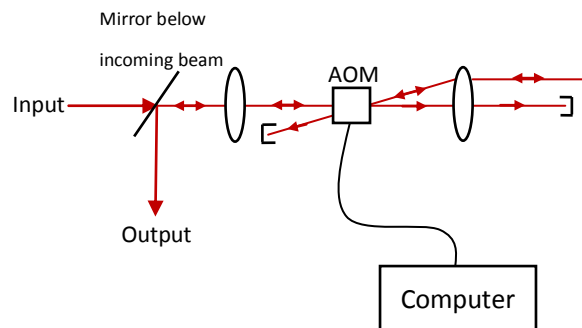


Figure 5.2 Pulse shaping system

There is a requirement on the burning pulses for creating spectral holes in the absorption profile. The output of the laser system, however, is a continuous wave. Therefore, a pulse shaping system is required.

This system comprises of an acousto-optic modulator (AOM), an arbitrary waveform generator and a computer. In the experiments, an sechyp pulse is used to achieve efficient transition between energy levels.[28] The pulse shape is created by Matlab in the computer and is sent to the AOM through an arbitrary waveform generator. The arbitrary waveform generator (2- channel 1GS/S Tektronix AWG520) which is connected to the computer through GPIB, controls the RF signal that is used to drive the AOM. By varying the RF signal, the phase, amplitude and frequency of the light can be shaped by the AOM. In the experiment, an AOM with a 200MHz center frequency is used in a double pass configuration, which cancels the spatial movement of the diffracted beam with frequency. Figure 5.2 demonstrates the arrangement of the pulse shaping system.

5.3 Crystal-Pr³⁺:Y₂SiO₅

There are two crystals which are used in different experiments, see figure 5.3. Both of them are Pr³⁺:Y₂SiO₅, with a praseodymium concentration of 0.05%.

In the high optical depth measurement, a crystal with the dimensions 10×10×12 mm is used. Light can go through every surface since there is no coating on any surface.

In the slow light experiment, a crystal with the dimensions 10×10×20 mm is used instead due to the demand of high optical depth. There are highly reflective coated surfaces except for a V-shape anti-reflection coated part where the light can enter and exit.(see Fig. 5.4) The light can propagate back and forth several times in the crystal. That means that the optical depth can be increased by many times.

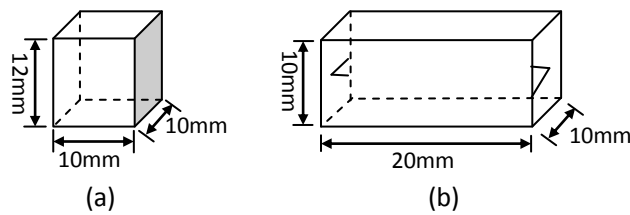


Figure 5.3 Two crystals are used in later experiments

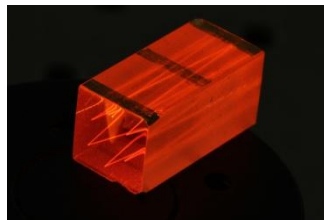


Figure 5.4 Display of the multipass crystal

5.4 Cryostat

The reason of the usage of a cryostat is that the attractive properties of the sample (Pr³⁺:Y₂SiO₅) such as long coherence time and inhomogeneous broadening arise at cryogenic temperatures. The cryostat which is used for holding the experimental crystal is a bath cryostat, which means the crystal can be submerged into the liquid helium. There are several interlayers inside the

cryostat. The outer layer is filled by liquid nitrogen and an inner one is designed for holding liquid helium. After that, a chamber is used to hold the sample. There is an auto needle valve which connects the sample chamber and the helium container. In the experiment, a temperature below 2.17K is needed to avoid bubbles, which appears at and above the boiling point of liquid helium. To lower the pressure, a vacuum pump is applied to evacuate the chamber to about 50mbar. At this pressure liquid helium to be superfluid.

Chapter 6

The experimental methods and setups

For different purposes, there are two different setups and methods. In this chapter, both of them will be described. First of all, the importance and the difficulty for measuring high αL will be discussed. Then a novel method will be presented to solve this. Moreover, as mentioned in Chapter 2 and 3, there are two goals to be achieved in the experimental part for slow light. One is to reduce the group velocity of light as much as possible. The other one is to evaluate the potential of high time delay-bandwidth product using the spectral hole burning technique with a $\text{Pr}^{3+}:\text{Y}_2\text{SiO}_5$ crystal. The method and the setup for achieving these purposes will be also given.

6.1 High αL measurement

6.1.1 The necessity and the difficulty for knowing high optical depth

Optical depth or optical thickness (αL) is presented in the Beer-Lambert law, which indicates the relation between the absorption of light and the properties of the material through the direction which the light propagates.

$$I_{\text{out}} = I_{\text{in}} e^{-\alpha L} \quad (\text{The Beer-Lambert Law})$$

In slow light experiments, the αL value is important for evaluating the slow light regime. That is because the theoretical value of group the velocity is in direct proportion to the width of the spectral hole, and in inversely proportional to the absorption coefficient. (See equation 2.15)

Thus, if we can measure the value of the optical depth, it is possible to compare the experimental result to the theoretical limitation. Moreover, an efficient quantum memory also needs a high αL , as this enhances the light-matter interaction.

Although high αL is required frequently and worth to be measured, there is no method that comes up for dealing with this. If the αL is large, for example 100, the output intensity is decreased by a factor of 3.7×10^{-44} . That means that there is hardly any light that travels through. It is extremely difficult to measure in a normal way.

6.1.2 A method to measure the αL value of $\text{Pr}^{3+}:\text{Y}_2\text{SiO}_5$ [31]

The relation between the polarization direction of the incident light and the dipole moment alignments determines the αL , which the light experiences when traveling through the medium. In a $\text{Pr}^{3+}:\text{Y}_2\text{SiO}_5$ crystal, there are two permanent dipole moments with an angle between them 24.8° , which are placed along one of the surfaces.[29] The orientations of dipole moments are shown in figure 6.1(a).

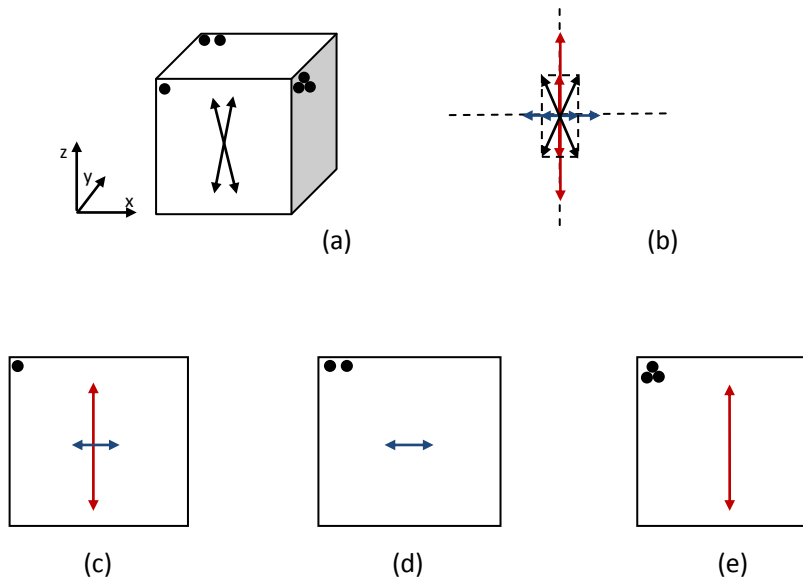


Figure 6.1 Schematic diagrams about dipole moments and the crystal.

Figure 6.1(b) shows an equal alignment after compounding the original dipole moments in another coordinate, as the red and blue lines. Figure 6.1(c) (d) and (e) indicate the components of the dipole moments aligned in each surface. Therefore, we can figure out that the maximum absorption can be obtained in both (d) and (e) by rotating the polarization direction of laser

beam along the red line. Moreover, the zero absorption can be achieved by tuning the polarization of the incident light vertically to the dipole moment both in (d) and (e).

If the incident beam is going through surface No.2 as in figure 6.1(d) with the polarization perpendicular to the dipole moment, the laser beam can go through the crystal without any absorption. We can then keep this polarization direction but rotate the crystal by a small angle around the x-axis. This can also be done by rotating the incident light instead of moving the crystal. As a result, the light will still not interact with the blue dipole moment. But it will interact with the red dipole moment since a component of this dipole moment will contribute to a small absorption. This geometry can be described in Figure 6.2. Because this absorption will be small, it can be measured.

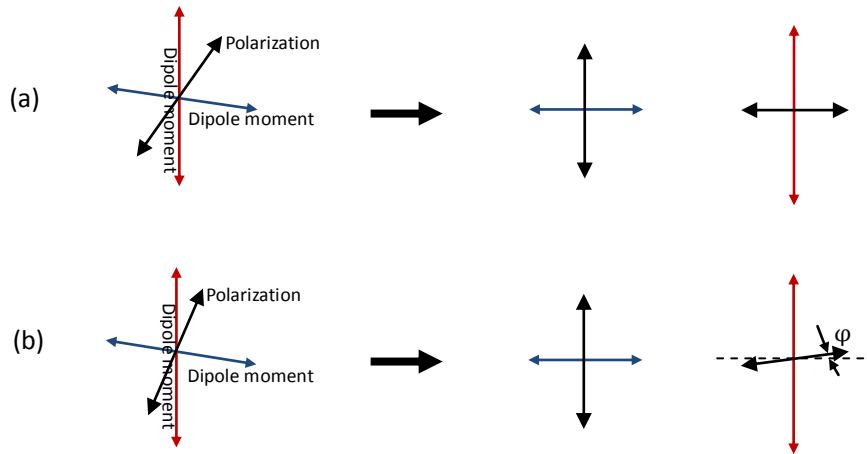


Figure 6.2 The geometric relations between polarization and dipole moments. (a) is in the original situation. (b) is the case after rotating the crystal or laser.

The maximum absorption can be obtained when the polarized direction fit the red dipole moment. Then the αL in figure 6.2 (b) can be expressed as

$$\alpha L_{\text{measure}} = \alpha L_{\text{Max}} \cdot \sin\varphi \quad (6.1)$$

Where $\alpha L_{\text{measure}}$ is the measured value of absorption after a tiny rotation of φ and αL_{Max} is the maximum absorption in the crystal.

Then the high αL can be calculated by

$$\alpha L_{\text{Max}} = \frac{\alpha L_{\text{measure}}}{\sin\phi} \quad (6.2)$$

6.1.3 The setup of high optical depth measurement

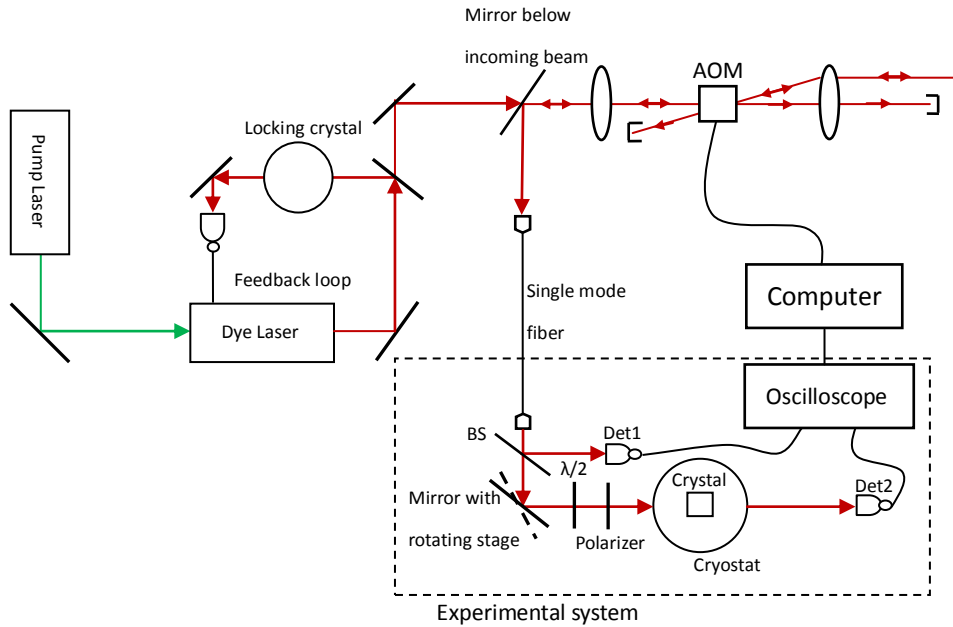


Figure 6.3 Optical alignments for high optical depth measurement.

The laser system and the pulse shaping system are the same as discussed in Chapter 5, and they are placed on an optical table in a clean room. The experimental system is aligned on another table, optically connected by a single mode fiber which is used for cleaning up spatial mode. A beam splitter then divides the light into two parts, one part of 4% percent intensity is detected by detector 1 as a reference, the other one with 96% intensity is sent to the sample. There is a mirror that can be tuned around the vertical axis, which is used for changing the incident angle to obtain a difference of absorption as discussed before. To expand the adjustable range, the distance between this mirror and the crystal should be shortened as much as possible. Otherwise, the incident light will miss the crystal or become blocked by the edge of the sample holder. A half lambda plate is used for rotating the polarization direction, and a linear polarizer is applied for making sure the light is linear polarized. It is very important to keep the polarization linear since only a tiny component can induce that we cannot obtain zero absorption.

6.2 Slow light experiment

6.2.1 To obtain slow light

Eq. (2.15) is an important equation for evaluating the group velocity of light in theory. The group velocity is proportional to the width of the spectral hole that is burned in the absorption profile and inversely proportional to the absorption coefficient. Therefore, we can imagine that if we burn an extremely narrow and very deep pit, then the group velocity will be reduced significantly. In the experiment, a 2MHz wide pit is burned in the center of the inhomogeneous profile for getting the deepest pit. Because the multipass crystal will change the interaction length (L), it will not influence the absorption coefficient. Therefore, only a single pass of the crystal is enough in this part.

6.2.2 To obtain high time delay-bandwidth product

As discussed in Chapter 3.3, Eq. (2.35) indicates the relation between time delay-bandwidth product and optical depth (αL). The time delay-bandwidth product is proportional to both the absorption coefficient (α) and the length (L). Therefore, the larger αL means the larger time delay-bandwidth product. The highest α can be obtained to go to the center of the inhomogeneous profile and the largest L can be achieved by going through the crystal many times (multipass). The estimated optical depth in the center of the profile is between 60 and 80.[30] Then the estimated value of time delay-bandwidth can be calculated by Eq. (2.35), which is between 4.8 and 6.4 in single pass. The maximum pass times are 12 in the crystal, which means the time delay-bandwidth can be improved 12 times. The estimated value then is between 57.6 and 76.8, which is much better than the results by using EIT, CPO and PSHB so far.

6.2.3 The setup of slow light

1) Slow light

The setup for getting slow light is the same as in figure 6.3. The only difference is that the crystal used in high αL measurement is crystal No. 1 as shown in figure 5.3 (a), this time crystal No.2 is used.

2) High time delay-bandwidth product

For obtaining the maximum value of that, the crystal should be used in a multipass alignment as [figure 5.4](#) shown. The incident beam and the output one pass the same surface after 12 passes in the crystal.

The setup in the experiment as indicated below in [figure 6.4](#).

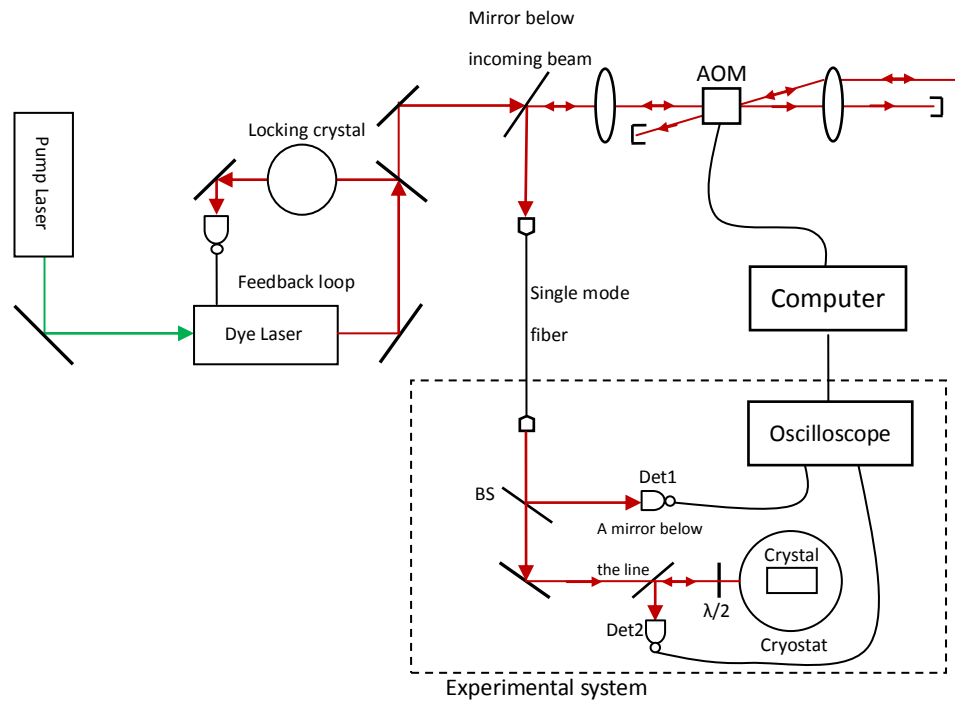


Figure 6.4 Optical alignments for obtaining high time delay-bandwidth product.

Chapter 7

The experimental results and discussions

In the chapter the results of the experiments will be given. To start with, the feasibility of the idea for measuring high αL will be experimentally tested. Next, the experimental data of the slow group velocity of light will be presented. In the end the results of time delay-bandwidth product will be shown.

7.1 The proof of the method using for measuring high αL

7.1.1 Results

As the [Figure 6.1](#) shown, entering perpendicular to the surface 1 in [figure 6.1 \(c\)](#) one cannot get zero absorption, but entering perpendicular to the surface 2([figure 6.1 \(d\)](#)) and surface 3([figure 6.1\(e\)](#)) it is possible. By comparing [figure 6.1\(d\)](#) and [figure 6.1\(e\)](#), entering surface 3 can give a larger absorption by aligning the polarization appropriately. Therefore, a test can be done by knowing which surface is which. This can be achieved by shining the laser perpendicular to each surface, coordinating with the half lambda plate and the polarizer. The surface 2 is chosen in the experiment since we can get a noticeable change when we rotate the incident angle of the laser beam.

Next, the incident beam was sent to the crystal vertically. By rotating the half lambda plate and

the polarizer, zero absorption was obtained. Then a small angle was added using the tuning mirror in figure 6.3. As discussed in Chapter 6.1, a small angle change between the light and the crystal will induce a difference in absorption. Then, the αL can be calculated by equation (6.2). Figure 7.1 indicates the situation when the light is vertically incident and the polarization is optimized for obtaining zero absorption. The laser frequency was at the edge of the inhomogeneous absorption. A 2 MHz spectral hole is made for observing the absorption change clearly. If the absorption is close to zero, we cannot see the pit shape. By changing the polarization the pit will come up. The absorption was measured by a readout sequence, which is proved that can be used to measure the small αL (below 2).

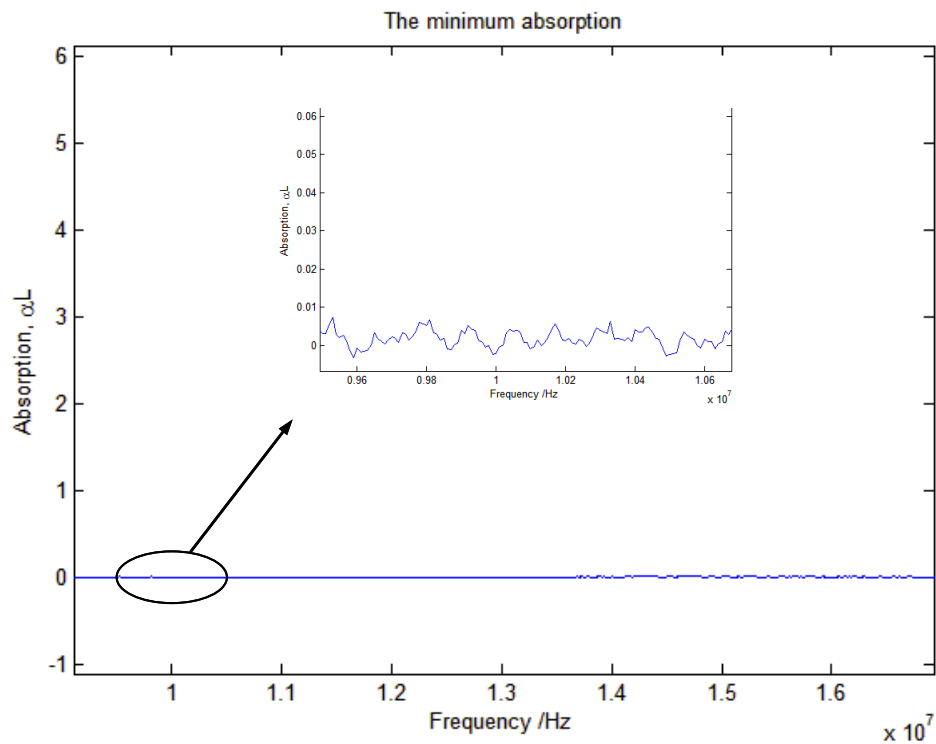


Figure 7.1 The absorption detected after creating a 2 MHz spectral pit when there is no absorption.

The situations after rotating a small angle of 5 minutes through the tuning mirror is shown in figure 7.2. And the average value also is calculated in the same area as that of figure 7.1 in figure 7.2, which are used for evaluating the absorption.

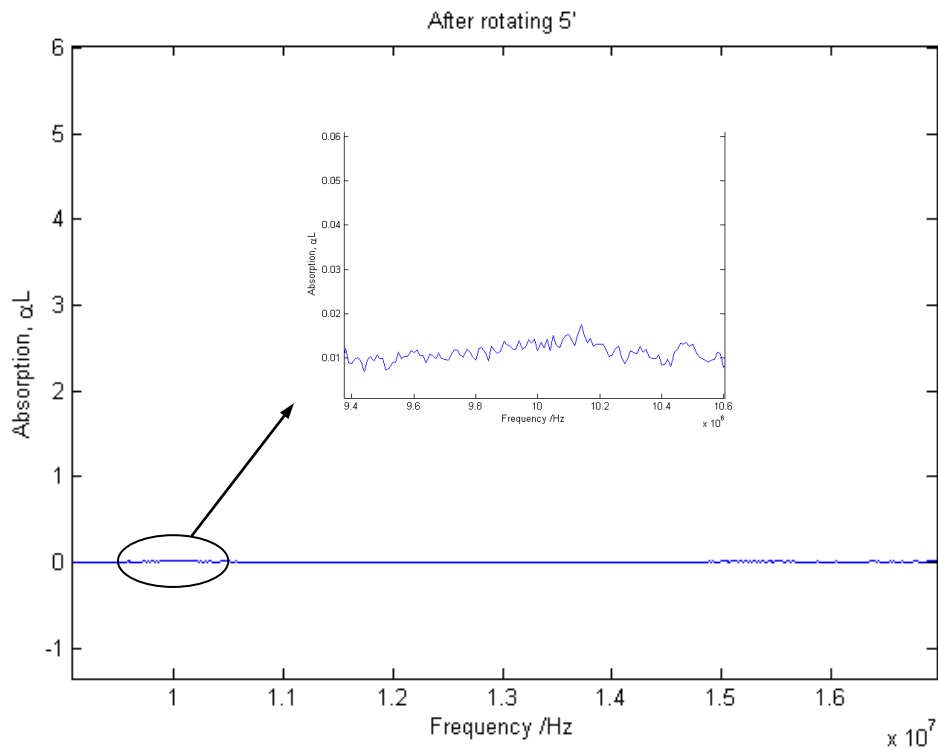


Figure 7.2 The situation after rotating the mirror 5 minutes

The average value between 9.5MHz and 10.5MHz in the circle region from [figure 7.1](#) was calculated as a reference.

$$\alpha L_0 = -0.00087$$

When the mirror rotates an angle of θ , the angle between light and the crystal get 2θ . Therefore, after rotating 5', the angle actually changes 10'. And the average value in the circle area is

$$\alpha L_{10'} = 0.01362$$

By applying equation (6.2), the αL can be calculated

$$\alpha L = \frac{\Delta\alpha L}{\sin\varphi} = \frac{\alpha L_{10'} - \alpha L_0}{\sin 10'} = 4.98$$

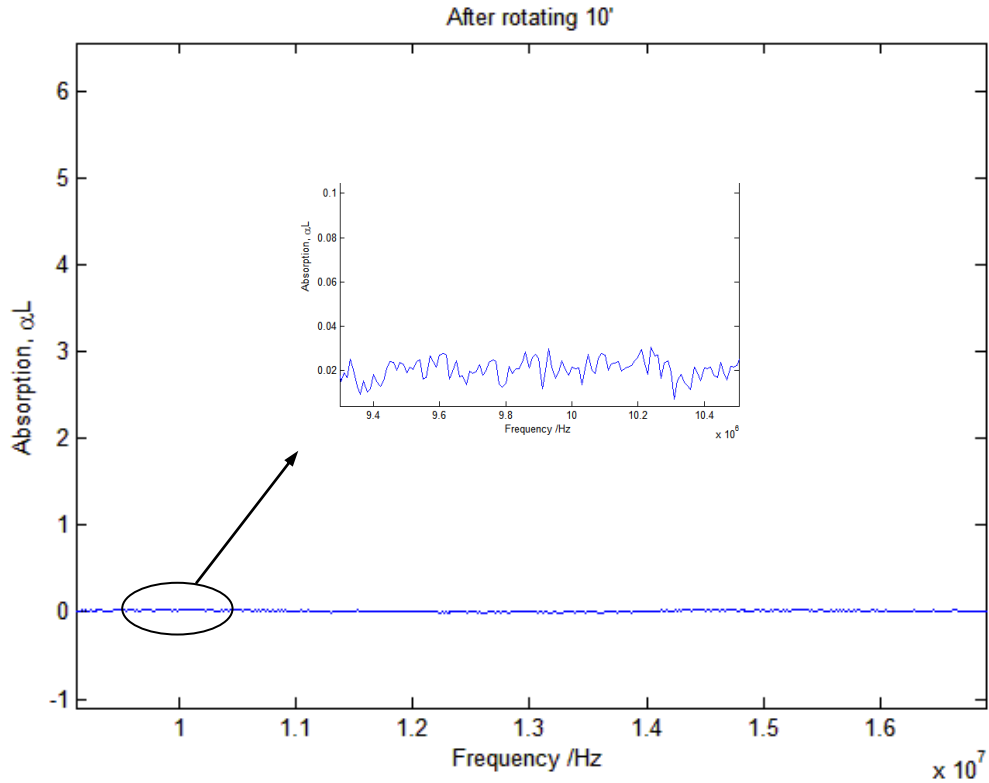


Figure 7.3 The situation after rotating the mirror 10 minutes

Then, a rotation of $10'$ was done to check if the last measurement is reliable. $2\varphi = 20'$

$$\alpha L_0 = -0.00087$$

$$\alpha L_{20'} = 0.02611$$

Therefore the αL is

$$\alpha L = \frac{\Delta\alpha L}{\sin\varphi} = \frac{\alpha L_{20'} - \alpha L_0}{\sin 20'} = 4.64$$

$$\overline{\alpha L} = \frac{4.98 + 4.64}{2} = 4.81$$

The error is $4.98 - 4.64 = 0.34$, which is $0.34 / \overline{\alpha L} = 7\%$.

The two different measurements got the answers in an acceptable error region. That means that this method is feasible.

$$\sigma = \sqrt{\frac{1}{n} \sum_{i=1}^n (\alpha L_i - \overline{\alpha L})^2} = \sqrt{\frac{0.17^2 + 0.17^2}{2}} = 0.17$$

$$\alpha L = 4.81 \pm 0.17$$

7.1.2 Discussion

A measurement of αL was done by rotating the mirror 5'. And another measurement was done to check the accuracy by tuning the mirror 10'. The laser frequency was adjusted to the edge of the inhomogeneous profile, so the αL is not so high. Moreover, the distance between the optical window of the cryostat and the sample as well as the dimensions of the crystal limited the adjustable angle, thus only two data have been obtained. However, we can already know the method is suitable for measuring high αL from the measurements.

7.2 Slow light experiment

7.2.1 Reduce the group velocity of light as much as possible

1) Result

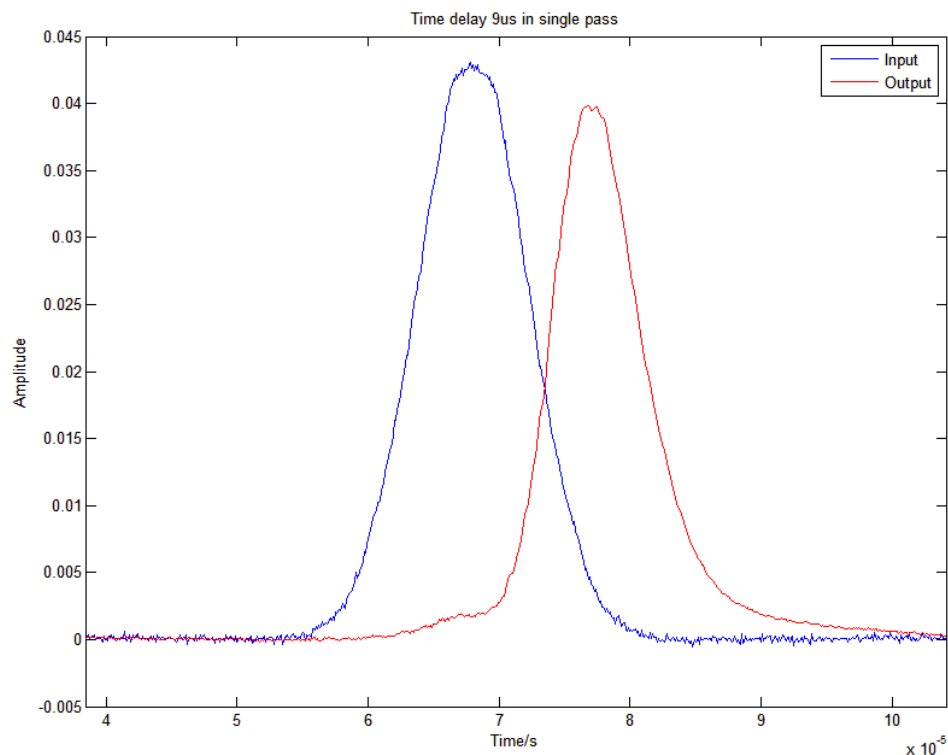


Figure 7.5 Slow light.

In this part, the laser went through the sample once. A 2MHz spectral hole was created. And then a Gaussian pulse with its FWHM of $10\mu\text{s}$ was sent to the middle of the hole. As figure 7.5 shown, the time delay between the input signal and the output one is $9.1\mu\text{s}$. The group velocity of light in

the sample can be calculated by

$$\frac{L}{v_g} - \frac{L}{c} = T_{\text{delay}}$$

$$v_g = \frac{1}{T_{\text{delay}} + L/c} = \frac{0.02}{9.1 \times 10^{-6} + 0.02/3.0 \times 10^8} = 2197.8 \text{ m/s}$$

2) Discussion

The result of group velocity was obtained in the experiment is the lowest one for achieving slow light by using spectral hole burning technique so far. As discussed in Chapter 2.2.3.3, the group velocity is determined by the width of the spectral hole as well as the absorption coefficient, see equation (2.15). Therefore, the velocity of light can be reduced by shortening the width and making the pit deeper. That means that the group velocity still has the potential to be reduced more.

7.2.2 Time delay-bandwidth product experiment

1) Results

(a) In the single-pass alignment

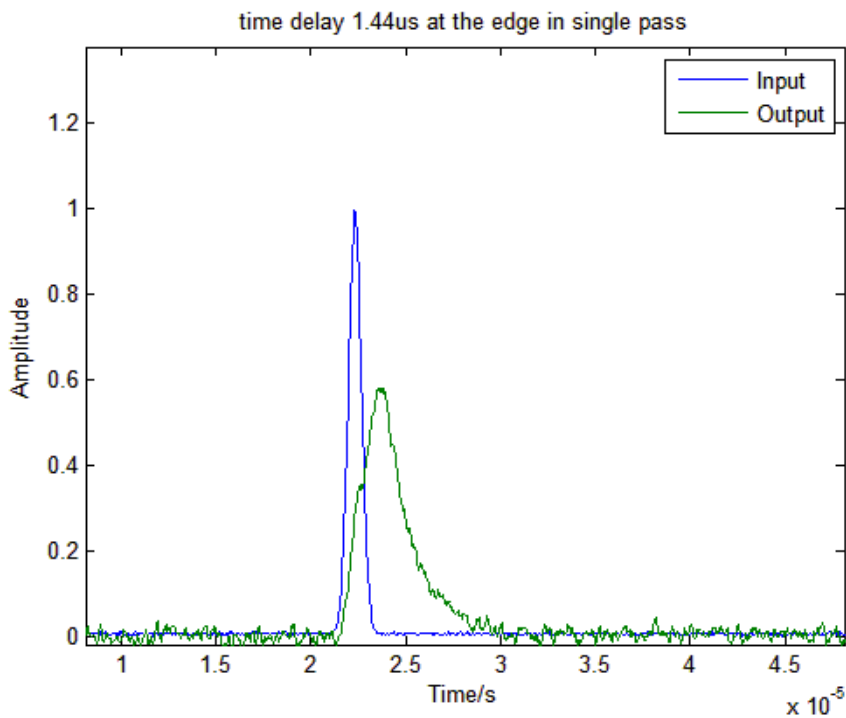


Figure 7.6 The situation of tuning the laser frequency to the edge of the inhomogeneous broadening

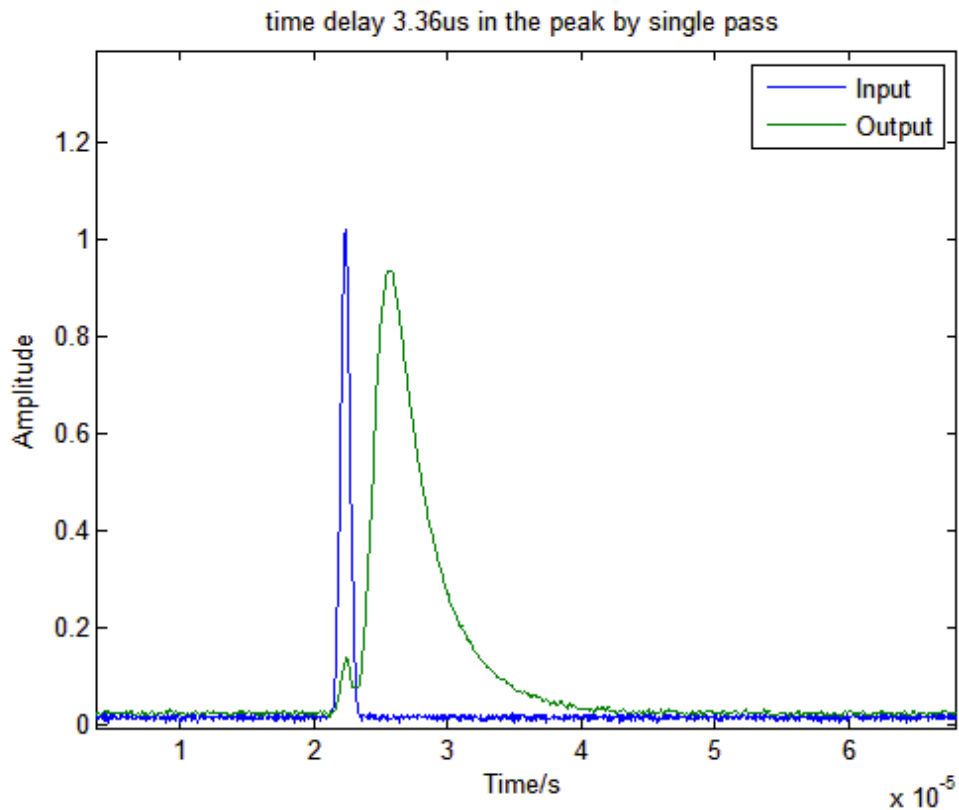


Figure 7.7 The situation of tuning the laser frequency to the center of the inhomogeneous broadening

The time delay-bandwidth product is proportional to $\alpha(\omega)L$. Therefore, there are two figures which are presented for comparing the change of DBP when varying the laser frequency.

The bandwidth of the packet is the fourier transform of the time duration.

Therefore, the DBP of figure 7.6 is

$$DBP_1 = T_{\text{delay}} \cdot B_{\text{packet}} = 1.44\mu\text{s} \cdot \frac{0.44}{2.4\mu\text{s}} = 0.264$$

The DBP if figure 7.7 is

$$DBP_2 = T_{\text{delay}} \cdot B_{\text{packet}} = 3.36\mu\text{s} \cdot \frac{0.44}{2.4\mu\text{s}} = 0.616$$

(b) In the multi-pass alignment

The multipass alignment was using in this part in order to increase the absorption, thus the time delay-bandwidth can be improved. Again, there are two figures, one of them indicates the case when the laser frequency at the edge of the inhomogeneous profile, the other one shows that when the frequency of the laser tuned to the center of the profile.

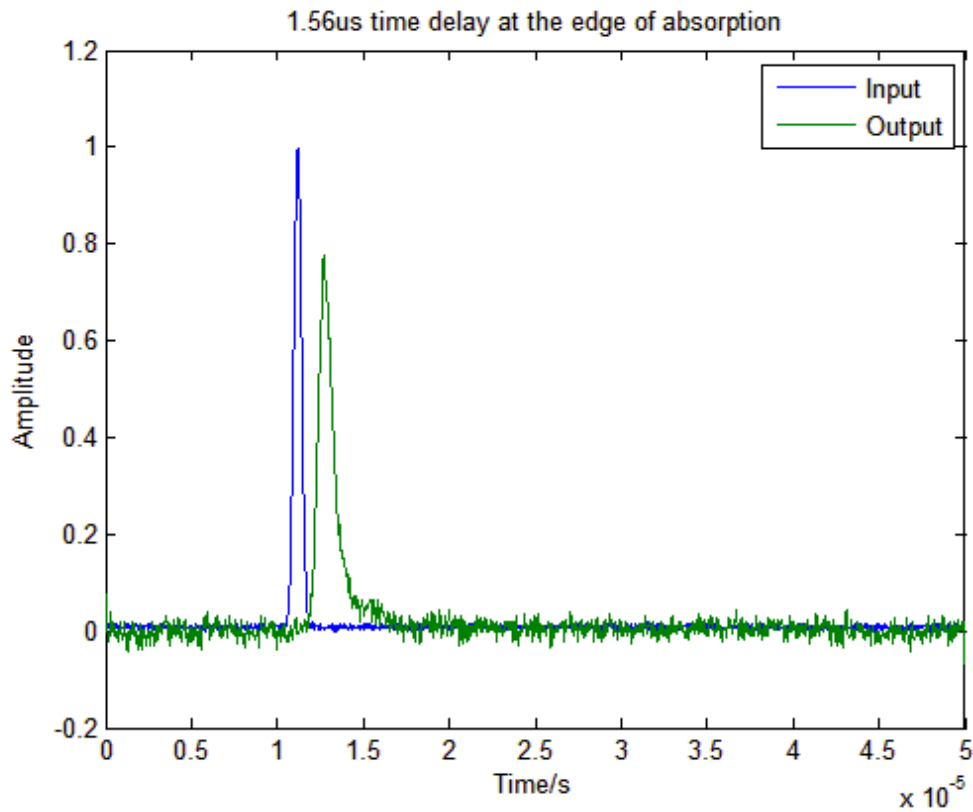


Figure 7.8 The situation of tuning the laser frequency to the edge of the inhomogeneous broadening by applying multipass of the sample

The DBP of [figure 7.8](#) is

$$DBP_3 = T_{\text{delay}} \cdot B_{\text{packet}} = 1.56\mu\text{s} \cdot \frac{0.44}{1.6\mu\text{s}} = 0.429$$

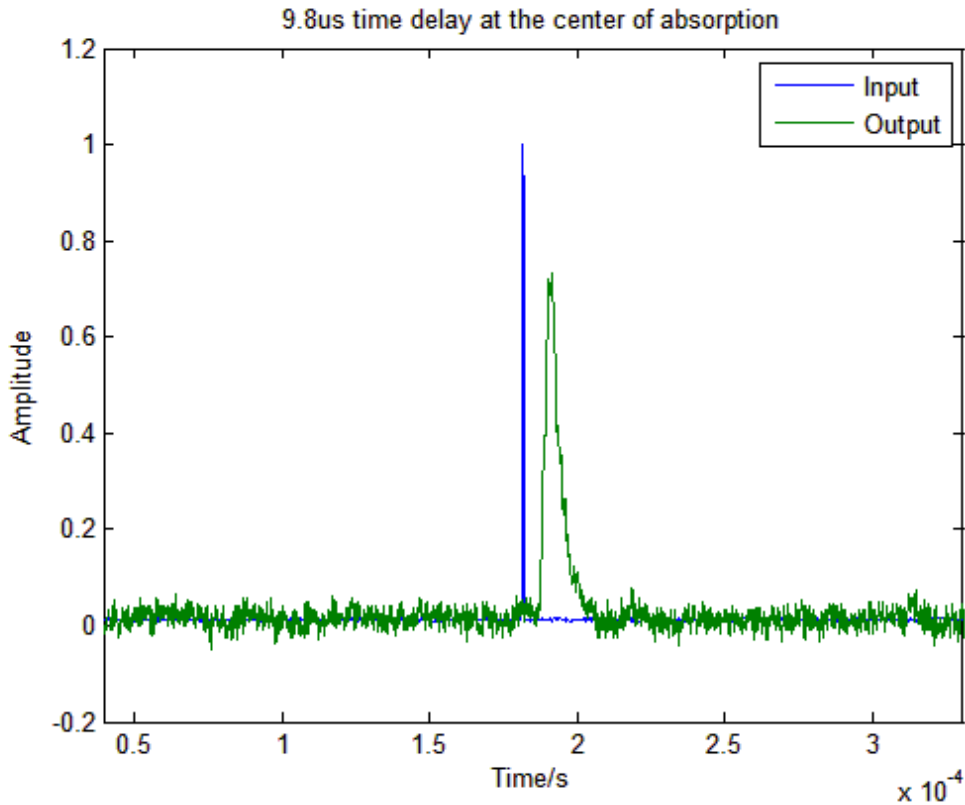


Figure 7.9 The situation of tuning the laser frequency to the center of the inhomogeneous broadening by applying multipass of the sample

The DBP of figure 7.8 is

$$DBP_4 = T_{\text{delay}} \cdot B_{\text{packet}} = 9.8\mu\text{s} \cdot \frac{0.44}{1.6\mu\text{s}} = 2.695$$

2) Discussion

The time delay-bandwidth product is determined by equation (2.35), which means the DBP increases when the $\Delta\alpha(\omega)L$ goes up. This relation was proved in the experiment both in the single pass alignment and the multipass alignment. By tuning the laser frequency from the edge of the inhomogeneous region to the center of that, DBP increased significantly. Also, when we changed the alignment from single pass to multipass, DBP increased too. The maximum DBP of single pass is 0.616 and that of multipass is 2.695.

However, we can see from the figures that the output light have a distortion, which limits the bandwidth. This happened due to the inefficient interaction of the light and the material. That

means that the spectral hole is not flat at its bottom, which induces the distortion.

Chapter 8

Conclusion and outlook

1. The idea for measuring high optical depth is tested and it is shown that it can be used.
2. The velocity of light reduced to 2197.8 m/s.
3. The maximum time delay-bandwidth product 2.695 using the multipass of the crystal.

The group velocity of light can be reduced by narrowing the pit (decrease Γ) or tailoring the edge of the pit (increase $\Delta\alpha$). **Figure 8.1** is an example of a narrower pit, which is 1MHz. And **Figure 8.2** shows a simulation of the situation after burning back two anti-holes to the edges of pit, which $\Delta\alpha$ increased significantly if compared with **figure 4.4**. The two ideas above that give the crystal experimental potentiality for obtaining a even slower group velocity.

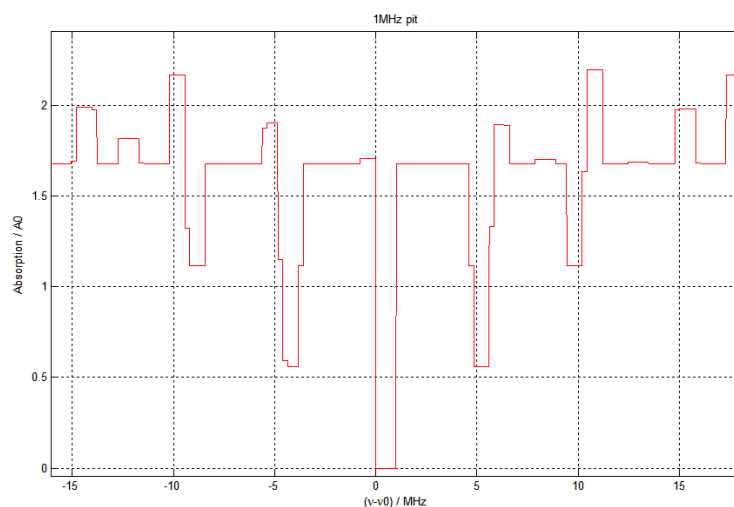


Figure 8.1 An example of a narrower pit

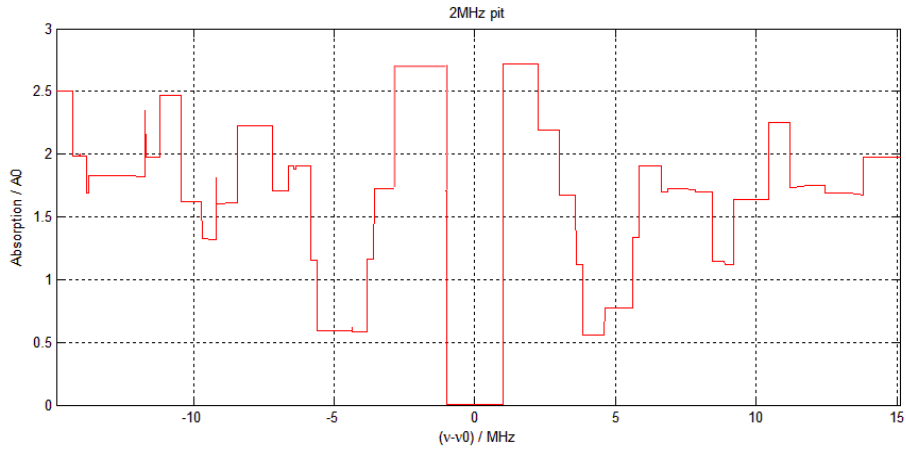


Figure 8.2 Increasing $\Delta\alpha$ by burning back anti-holes

For high time delay-bandwidth, a pit with a flat bottom is needed for optimizing the performance. The problem is that much more laser fluence is needed for creating an empty pit when the optical depth increases 12 times. This problem needs to be addressed in the future. The estimated value of DBP in this crystal after 12 times' passes is between 57.6 and 76.8. Therefore, there is a lot of potential to get higher value.

The size of slow light buffer is also an important thing needs to be considered. Take a single-wavelength optical fiber delay line as an example, the length of that should be about 40Gm for obtaining the same performance of a normal electric router, which is unpractical to be achieved. [20] But multipass alignment can solve this.

The sample has very brilliant properties when aligned for multipassing such as extremely high αL , which is important for obtaining high time delay-bandwidth, and it is also an important factor for achieving higher quantum memory efficiency in quantum information group later on. The procedure of doing this can be found in Appendix B.

Acknowledgements

First of all, I would like to sincerely thank my supervisor Stefan Kröll for sharing me his profound knowledge and for always having time for discussions. Many thanks to Mahmood, Atia and Yan, experiments cannot be fluent without the supporting provided by them. I especially would thank to Lars Ripple for sharing his astonishing experimental experience and many smart ideas. I also like to thank all the rest members in quantum information group Samuel, Prathamesh and Jenny, as well as an old member, Felix, for a good atmosphere.

I would like to thank my supervisor of the photonics programme Anne L'Huillier for accepting me as a master student in this fascinating division.

Finally, I would like to thank my dear parents for their patience and support during my studies.

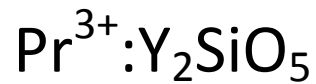
Bibliography

- [1] Yixin Chen, Yide Yu. *'The applications of slow light and optical memory in quantum information'*. Chinese Journal of Physics,30(5), (2008)
- [2] B.E.A.Saleh, M.C.Tech. *Fndamentals of Photonics, 2nd Edition*. A John Wiley & Sons Inc., New Jersey(2007)
- [3] Brillouin, Léon. *Wave Propagation and Group Velocity*. Academic Press Inc., New York (1960)
- [4] Clayton R. Paul, *Analysis of Multiconductor Transmission Lines*. John Wiley & Sons., New York (1994)
- [5] G. Diener. Super luminal group velocities and information transfer. Phys.Lett.A 223,327 (1996).
- [6] Valerio Lucarini, Jarkko J. Saarinen, Kai-Erik Peiponen and Erik M. Vartiainen. *Kramers-Kronig relations in Optical Materials Research*, Springer, Heidelberg(2005)
- [7] S. E. Harris ,J.E.Field and A. Imamoglu. *'Nonlinear optical processes using electromagnetically induced transparency'*. Phys. Rev. Lett., 1990, 64(10): 1107 -1110
- [8] Scully M. O. and Zubairy M. S. *Quantum Optics*. Cambridge: Cambridge University Press, 1997
- [9] Hau L V, Harris S E, Zachary Dutton, Cyrus H. Behroozi. *'Light speed reduction to 17 metres per second in a ultracold atomic gas'*. Nature,1999,397:6720
- [10] Kash M. M., Sautenkov V. A., Zibrov A. S., Hollberg L., Welch G. R., Lukin M. D., Rostovtsev Y., Fry E.S. and Scully M. O. *'Ultraslow group velocity and enhanced nonlinear optical effects in coherently driven hot atomic gas'*. Phys. Rev. Lett., 1999, 82(26): 5229-5232
- [11] Budker D. et al., *'Nonlinear magneto-optics and reduced group velocity of light in atomic vapor with slow ground state relaxation'*. Phys. Rev. Lett., 1999, 83(9):1767-1770
- [12] Turukhin A. V. et al., *'Observation of ultraslow and stored light pulses in a solid'*. Phys. Rev. Lett., 2002, 88(2): 023602
- [13] S. E. Schwartz and T. Y. Tan, *'Wave interactions in saturable absorbers'*. Appl. Phys. Lett. 10,4 (1967).
- [14] M. S. Bigelow, N. N. Lepeshkin ,and R. W. Boyd, *'Observation of Ultraslow Light Propagation in a Ruby Crystal at Room Temperature'*. Phys. Rev. Lett. 90,113903 (2003).
- [15] E. Baldit, K. Bencheikh, P. Monnier, J. A. Levenson, and V. Rouget, *'Ultraslow Light Propagation in an Inhomogeneously Broadened Rare-Earth-Ion-Doped Crystal'*. Phys. Rev. Lett. 95,143601 (2005).
- [16] R. Yano, M. Mitsunaga, and N. Uesugi, *'Nonlinear laser spectroscopy of $\text{Eu}^{3+}:\text{Y}_2\text{SiO}_5$ and its application to time-domain optical memory'*, J.Opt.Soc.Am.B 9, 992-997 (1992)
- [17] R. N. Shakhmurov, A. Rebane, P. Mégret, and J. Odeurs, *'Slow light with persistent hole*

- burning*, Phys.Rev.A, 71, 053811 (2005).
- [18] A. Rebane, R. N. Shakhmurov, P. Mégret, and J. Odeurs, '*Slow light with persistent spectral hole burning in waveguides*'. J. Lumin. 127,22 (2007).
- [19] R. Lauro, T. Chanelière, and J. L. LeGouët. '*Slow light using spectral hole burning in a Tm³⁺-doped yttrium-aluminum-garnet crystal*'. Phys.Rev.A 79,063844 (2009)
- [20] Rodney S. Tucker, Pei-Cheng Ku, and Constance J. Chang-Hasnain, '*Slow-Light Optical Buffers: Capabilities and Fundamental Limitations*'. J. Lightwave Technol. 23, 4046- (2005)
- [21] R. S. Tucker, P. C. Ku, and C. J. Chang-Hasnain, '*Delay-bandwidth product and storage density in slow-light optical buffers*'. Elect. Lett. 41, 208-209 (2005).
- [22] Liu C, Dutton Z, Behroozi CH, Hau LV. '*Observation of coherent optical information storage in an atomic medium using halted light pulses*'. Nature. 409(6819):490-3.(2001)
- [23] Pei-Cheng Ku, Forrest Sedgwick, Connie J. Chang-Hasnain, Phedon Palinginis, Tao Li, Hailin Wang, Shu-Wei Chang, and Shun-Lien Chuang, "*Slow light in semiconductor quantum wells*," Opt. Lett. 29, 2291-2293 (2004)
- [24] E. Fraval, M. J. Sellars, and J. J. Longdell, '*Method of extending hyperfine coherence times in Pr³⁺:Y₂SiO₅*'. Phys. Rev. Lett. 92(7):077601(2004).
- [25] E. Fraval, M. J. Sellars, and J. J. Longdell, '*Dynamic Decoherence Control of a Solid-State Nuclear-Quadrupole Qubit*'. Phys. Rev. Lett. 95, 030506 (2005)
- [26] L.Rippe. '*Quantum Computing with Naturally Tapped Sub-Nanometre-Spaced Ions*'. PhD thesis, Division of Atomic Physics, LTH (2006).
- [27] B.Julsgaard, L. Rippe, A. Walther and Stefan Kroll. '*Understanding laser stabilization using spectral hole burning*'. Optics Express, 15,11444(2007)
- [28] Andreas Walther. '*Coherent processes in rare-earth-ion-doped solids*'. PhD thesis, Division of Atomic Physics, LTH (2009).
- [29] F. R. Graf, A. Renn, G. Zumofen and U. P. Wild. '*Photo-echo attenuation by dynamical processes in rare-earth-ion-doped crystals*'. Phys.Rev.B 58,5462-5478(1978)
- [30] A. Walther, A. Amari, S. Kroll and A. Kalachev. '*Experimental superradiance and slow-light effects for quantum memories*'. Phys. Rev. A, 80, 012317 (2009)
- [31] Personal communication with Lars Rippe.

Appendix A

The procedure for measuring the αL in



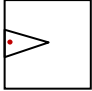
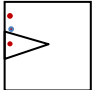
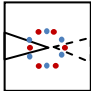
1. Make sure how the dipole moment direction aligned in each surface of the crystal.
2. Clarify the surfaces in practical.
3. Choose one surface which only has one dipole moment.
4. Shoot the laser vertically. (overlap the reflective light with the incident light)
5. Rotate the half lambda plate to obtain a minimum absorption.
6. Apply a polarizer to clean up the polarization and tune to the zero absorption.
7. Rotate the mirror in a small angle and record this angle of φ . Record the absorption difference $\Delta\alpha L$
8. Calculate the value of αL through the relations which has been shown in Chapter 6.1

Notice:

1. The distance between adjustable mirror and the sample should as short as possible.
2. When the mirror rotates by φ , the actual angle changes 2φ .

Appendix B

Adjustment for obtaining multipass in the coating crystal

- (a)  Shoot the beam vertically to the surface
- (b)  Adjust the mirror by the horizontal axis to get a reflection like the picture.
- (c)  Adjust the mirror by the vertical axis to get such a reflective pattern.

Red points indicate the reflective points at the front surface and the blue ones express the reflective points at the back surface. The hard V-shape shows the anti-coated part for passing the light at the front surface and the dash one indicates that at the back surface.

After successfully adjusting, a pattern likes the figure below can be seen from the back side of the optical window, without any point obvious brighter than other.

